Click Here for Full Article

Comparison of local energy conversion estimates from Cluster with global MHD simulations

L. Rosenqvist,[1] H. J. Opgenoorth,[2] L. Rastaetter,[3] A. Vaivads,[1] I. Dandouras,[4] and S. Buchert[1]

Received 29 August 2008; revised 23 September 2008; accepted 7 October 2008; published 8 November 2008.

[1] The local energy conversion across the magnetopause has been estimated with Cluster for two magnetopause crossings. A load region, conversion from magnetic to particle energy, was identified on the dayside high-latitude magnetopause during south/dawnward IMF. Another crossing of the dawn flank magnetotail during dominantly duskward IMF was identified as a generator region where the magnetosphere is loaded with magnetic energy. The observations have been compared to results of the BATS-R-US global MHD simulation based on observed IMF conditions. BATS-R-US reproduced the magnetopause regions crossed by Cluster as a load and a generator region, correspondingly. The magnitude of the estimated energy conversion from Cluster and the model are in quite good agreement. BATS-R-US cannot reproduce the observed sharp magnetopause and some topological differences between the observations and the model occur.

Citation: Rosenqvist, L., H. J. Opgenoorth, L. Rastaetter, A. Vaivads, I. Dandouras, and S. Buchert (2008), Comparison of local energy conversion estimates from Cluster with global MHD simulations, *Geophys. Res. Lett.*, *35*, L21104, doi:10.1029/2008GL035854.

1. Introduction

[2] It is well known that during periods of southward interplanetary magnetic field (IMF) the energy coupling between the solar wind (SW) and the Earth magnetosphere (MSPH) is considerably enhanced. This can best be explained by a reconnection process occurring in the sub-solar region. In the vicinity of the reconnection region the release of magnetic energy accelerates particles producing high-speed reconnection jets in load regions on the magnetopause (MP). The energy flow into the MSPH is driven as the reconnected field lines convect with the SW flow around the MP. At the MP, generator regions form where the magnetic tension force breaks the SW flow and the MSPH is loaded with magnetic energy at the expense of the solar wind kinetic energy. Figure 1 illustrates the extent of MP load and generator regions for typical southward IMF conditions.

[3] Due to lack of global measurements the overall energy transfer into the MSPH is commonly determined from empirical proxies [e.g., *Akasofu*, 1979]. However, recently *Rosenqvist et al.* [2008] used Cluster observations to obtain the local power conversion (Q) across the MP from the observed quantities based on the following relation

$$Q\left(Wm^{-2}\right) = \int \underbrace{\left(\vec{j} \times \vec{B}\right) \cdot \vec{v}}_{= \vec{E} \cdot \vec{j} \text{ in ideal MHD}} \quad |\vec{v}_{mp} - \vec{v}_{sc}| \mathrm{d}t \qquad (1)$$

where v_{mp} is the MP velocity, v_{sc} the spacecraft velocity and $\mathrm{d}x = |\vec{v}_{mp}\text{-}\vec{v}_{sc}|\ \mathrm{d}t$ represents the MP width. Generally $v_{mp} > v_{sc}$ and the second term can be neglected. This relation represents the conversion between magnetic and kinetic (thermal and bulk flow) energy. The value and also sign of the power conversion depends on the reference frame. The power conversion can be divided into the contributions due to expansion/contraction of the MP and due to gains or losses in the MP reference frame. The contribution from MP motion is difficult to determine and we neglect it assuming that the motion of the MP is an approximately adiabatic process. The Lorentz force entering this equation can be separated into two parts,

$$\vec{j} \times \vec{B} = \nabla \cdot \vec{T}_s - \nabla\left(\frac{B^2}{2\mu_0}\right), \qquad (2)$$

the first term corresponding to a magnetic tension force and the second to the magnetic pressure gradient force. The global energy transfer into the MSPH can be obtained by extrapolating the local Cluster observations assuming a function of its spatial dependence over the MP. This has been done during the Halloween storm the 30th of October 2003 by *Rosenqvist et al.* [2006].

[4] On the other hand, global magnetohydrodynamic (MHD) simulations provide a means to investigate both the global and local energy transfer in the SW-MSPH system. *Palmroth et al.* [2003] used, for the first time, energy transfer estimates from global MHD simulations to investigate locations on the MP surface where significant energy transfer took place during the evolution of a major geomagnetic storm. They calculate the total energy flux component normal to the MP surface, thus giving the energy flux transferred from the SW to the MSPH. Recently, *Laitinen et al.* [2007] used a method equivalent to the one described in this paper based on energy conversion determined from the divergence of the Poynting flux ($\nabla \cdot \vec{S}$) which in steady state equals $-\vec{E} \cdot \vec{j}$. However, although models are important tools for investigating SW-MSPH coupling they must continuously be verified by in-situ

[1] Swedish Institute of Space Physics, Uppsala, Sweden.
[2] Solar System Mission Division, ESTEC, ESA, Noordwijk, Netherlands.
[3] Space Weather Laboratory, NASA Goddard Space Flight Center, Greenbelt, Maryland, USA.
[4] CESR, Toulouse, France.

0094-8276/08/2008GL035854$05.00

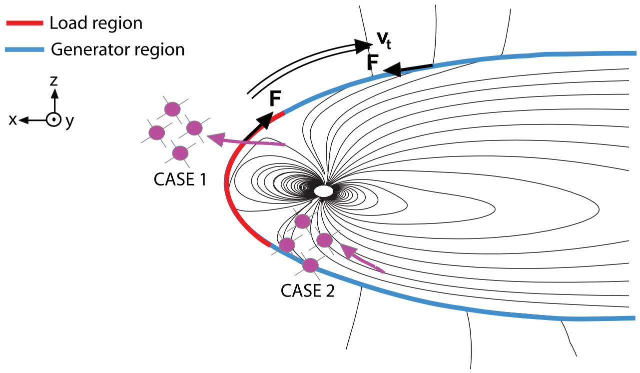

Figure 1. A schematic sketch of load/generator regions around the MP during southward IMF and the location of Cluster (pink arrows represent Cluster trajectories) for the load (CASE 1) and generator (CASE 2) region.

observations to validate the accuracy of the information they provide.

[5] In this study we investigate whether a commonly used global MHD model BATS-R-US can, indeed, reproduce the detailed local observations made by Cluster. Two different MP crossings corresponding to a load (Case 1) and generator (Case 2) region, respectively, as identified by Cluster observations have been compared with model results (see Figure 1).

2. Model and Instruments

[6] The magnetospheric MHD simulation that has been used in this study is the BATS-R-US model [*Powell et al.*, 1999; *Gombosi et al.*, 2002]. The BATS-R-US code solves the MHD equations in 3-D assuming ideal MHD (zero resistivity). BATS-R-US uses an adaptive grid composed of rectangular blocks with varying degrees of spatial refinement. The finest resolution of 0.25 R_E is used at the location of comparison with Cluster observations. The upstream inflow boundary at X = 33 R_E is updated with ACE solar wind and interplanetary data propagated to the sunward boundary of the simulation domain. The model output is saved every 60 seconds.

[7] The model results are compared to observations from the Cluster satellites [*Escoubet et al.*, 2001, and references therein]. We have used data from the FGM and CIS instruments.

3. Results

3.1. Case 1: Load

[8] On the 26th of January, 2001, Cluster observed multiple dayside MP crossings (Case 1) in the high-latitude northern hemisphere ([X_{GSM}, Y_{GSM}, Z_{GSM}] = [4.9, 7.1, 9.7] R_E at 10:39 UT) characterized by high speed reconnection jets [e.g., *Phan et al.*, 2004]. The interplanetary conditions (south/dawnward) were very steady during the period of the crossings [see *Phan et al.*, 2004]. *Rosenqvist et al.* [2008] found, using Cluster observations and equation (1), that the majority of the crossings corresponded to loads. For details on the estimation of the power conversion, see *Rosenqvist et al.* [2008].

[9] Figure 2 shows the simulation result for 26th January, 2001, at 10:39 UT in a cut in the Y_{GSM} = 7.2 R_E plane, the Y-position of Cluster. The color coding shows the power conversion, $\vec{E} \cdot \vec{j}$ estimates, which in ideal MHD correspond exactly to $(\vec{j} \times \vec{B}) \cdot \vec{v}$ which we have calculated from Cluster observations. Red color corresponds to positive Q and thus load regions while blue corresponds to negative Q and generator regions. The bowshock is easily identified as the blue bullet shaped boundary region in front of the MSPH. Also, we can directly see that the dayside MP corresponds to a load region. The magnetic field shape is shown in Figure 2 where black lines correspond to open field-lines, red correspond to closed field lines, and blue to the IMF. The arrows show the magnetic field direction in the X–Z plane.

[10] In order to compare the model estimates with Cluster observations we need to integrate the model results across the width of the MP at the location of Cluster. The real location of Cluster is marked with a black arrow in Figure 2. However, in the model this region appears to correspond to an exterior cusp region and hence an open field line configuration. It is evident from ion measurements that Cluster observes the high-energy ion population in the dayside plasma sheet on closed field-lines [see *Phan et al.*, 2004, Figure 2d]. Therefore, for comparative reasons we must artificially lower the Cluster location in the model to Z_{GSM} = 5 R_E (grey arrow in Figure 2). This corresponds to an neighboring closed field-line region which are in good agreement with the Cluster data. Figure 3a shows a zoomed in view of the model $\vec{E} \cdot \vec{j}$ estimates in the Z_{GSM} = 5 R_E plane and the region of the chosen equivalent Cluster location. We have integrated $\vec{E} \cdot \vec{j}$ along the MP normal (shown as black arrow in Figure 3a) as estimated with

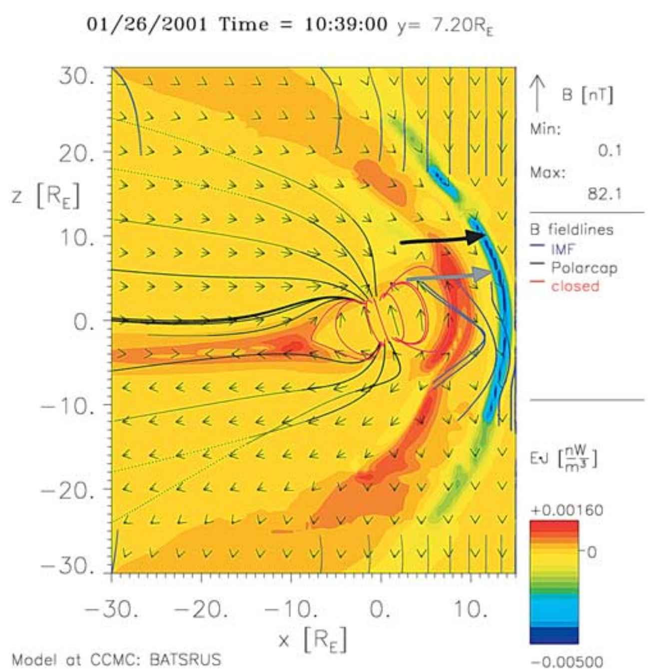

Figure 2. A cut of the modeled MSPH on 26 January 2001 in the Y = 7.2 R_E plane where Cluster is located. The colour coding shows $\vec{E} \cdot \vec{j}$ estimates and vector flow lines of B_x and B_z.

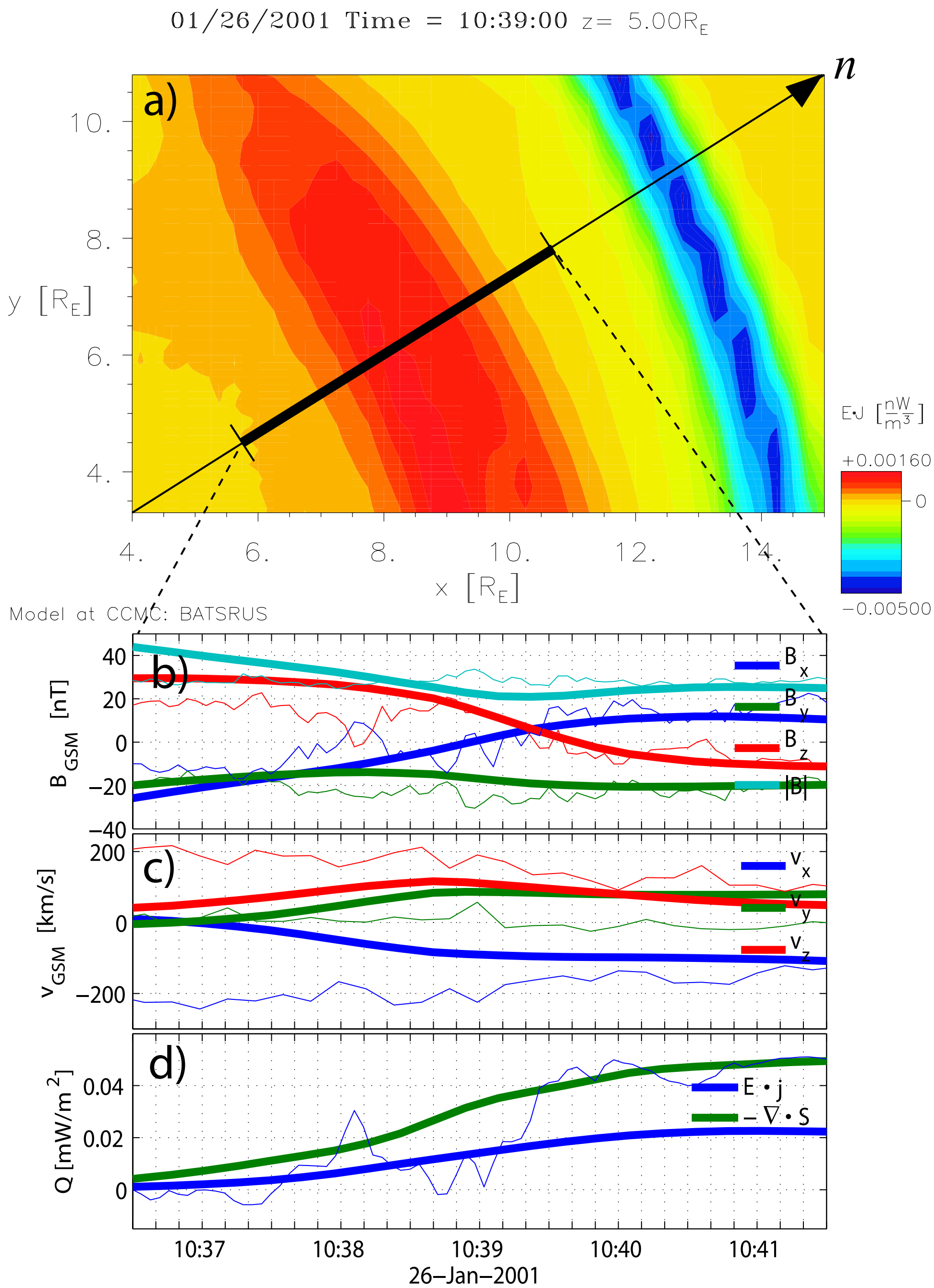

Figure 3. Comparison of Cluster and BATS-R-US model results for the load case, 26 January 2001. (a) A zoomed view of Figure 2 now in the $Z = 5$ R_E plane. (b) Magnetic field and (c) velocity components in GSM coordinates and (d) the power conversion across the MP. The thick lines corresponds to BATS-R-US estimates and the thin lines to Cluster observations.

minimum variance technique (MVA), n_{GSM} = [0.62, 0.49, 0.61], from Cluster observations (for further details, see *Rosenqvist et al.* [2008]). The MP boundary in the model is identified by a strong peak of the electric current density and a gradient of the plasma density as the configuration is changed from the low density MSPH to the high density magnetosheath (MSH) (not shown).

[11] In the case of the Cluster observations, v_{mp} is used to convert from temporal to spatial scales to integrate across the MP width. In the case of numerical simulations the integral can be estimated directly at the time of the current sheet crossing as observed by Cluster (10:39 UT) by integrating along the thick black line in Figure 3. However, in the model the MP is stationary ($v_{mp} \approx 0$), thus an artificial spacecraft speed of 100 km/s is chosen such that it takes the same time to cross the MP as for real satellites. The high artificial spacecraft speed reflects the fact that the width of the MP transition region in the simulation is not as sharp as in observations due to the limitations of solving the MHD equations on a finite-resolution grid. However, the assump-

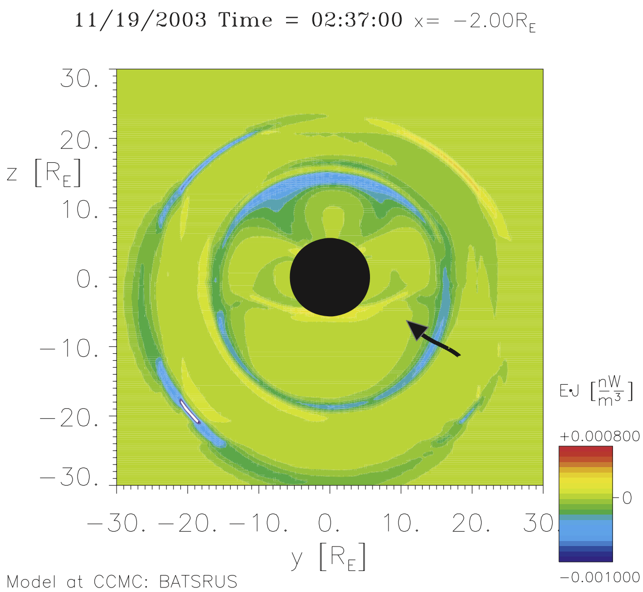

Figure 4. A cut of the modeled MSPH on 19 November 2003 in the $X = -2$ R_E plane where Cluster is located. The colour coding shows $\vec{E} \cdot \vec{j}$ estimates.

tion of this speed is not critical as it does not affect the magnitude of the power conversion as it is canceled in the integration $((\vec{E} \cdot \vec{j})\, v_{mp} \Delta t = (\vec{E} \cdot \vec{j}) v_{mp} \frac{\Delta x}{v_{mp}} = (\vec{E} \cdot \vec{j})\, \Delta x)$.

[12] Figure 3b shows that the magnetic field comparison is rather good between the model and Cluster as well as the model can reproduce the velocity observations (Figure 3c) in the MSH. The deviations between the model estimates and Cluster observations of the velocity in the MSPH might be due to the fact that the model cannot represent reconnection jets on the magnetospheric side of the MP. Figure 3d shows the estimated power conversion across the MP and the trends are very similar between the observed and modeled curve (blue line). For comparative reasons we have also added the power conversion deduced from $-\nabla \cdot \vec{S}$ from BATS-R-US (green line) as used by *Laitinen et al.* [2007] and it is a factor two higher than the modeled $\vec{E} \cdot \vec{j}$. This discrepancy between $-\nabla\, \vec{S}$ and $\vec{E} \cdot \vec{j}$ from the model cannot be explained by temporal changes in the modeled magnetic field (not shown). Instead, it is most probably due to numerical dissipation in the MHD code at the MP. However, it is not clear how this affects the two different quantities and thus it is not clear which of the quantities, $-\nabla \cdot \vec{S}$ and $\vec{E} \cdot \vec{j}$, should be compared to the observations.

3.2. Case 2: Generator

[13] For comparison and contrast in this study a generator event was identified on the 19th of November 2003, when Cluster observed the tailward flank of the MP, $[X_{GSM}, Y_{GSM}, Z_{GSM}] = [-2, 15.3, -10.1]$ R_E, at 02:37 UT. The interplanetary magnetic field was predominantly duskward, $B_y = 1.3$ nT and $B_z = 0.1$ nT, at this time according to time-shifted ACE observations using a minimum variance technique developed by *Weimer et al.* [2003]. The local power conversion has been estimated on the basis of equation (1). The current density was estimated with the curlometer technique and the MP velocity $v_{mp} = 70$ km/s was estimated by timing magnetic field measurements among 4 spacecraft.

[14] Figure 4 shows the simulation result for 19th January, 2003, at 02:37 UT in a cut in the $X_{GSM} = -2$ R_E plane at the Cluster location. The color coding is identical to that explained above, although the scale is different for this event. The black arrow illustrates the location of Cluster and it is evident that the MP acts as a generator at this location (blue corresponding to negative Q).

[15] Again, the method to compare the model with Cluster is identical to what has been described for the load case above. However, for this case the discrepancy between the observed and modeled MP thickness was even larger, thus the artificial spacecraft velocity used for this case corresponds to 600 km/s. The normal has been estimated with both MVA and 4-sc timing methods, resulting in very similar results (MVA giving $n_{GSM} = [0.13, 0.40, -0.91]$). Figure 5 is identical to Figure 3 but for the current case. Note, that Cluster observes first the MSH and then the MSPH, thus we have integrated from right to left in Figure 5a. The model reproduces both the magnetic field and velocity measurements by Cluster very well (Figures 5b and 5c).

[16] The modeled power conversion, $\vec{E} \cdot \vec{j}$, in Figure 5d shows that the MP acts as a generator. For this event $-\nabla \cdot \vec{S}$ and $\vec{E} \cdot \vec{j}$ agree well as we are not in the vicinity of a reconnection site and thus most probably much less affected by numerical dissipation effects. The equivalent Cluster estimate, the scalar $(\vec{j} \times \vec{B}) \cdot \vec{v}$ shown as the green line, corresponds to a load instead. However, if we only take the tangential velocity component into account, as done in earlier studies, the Cluster estimate (blue line) corresponds to a generator. This discrepancy might be due to the fact that we are going from a very small magnetic field strength in the MSH to a very large magnetic field strength in the MSPH which results in a very large contribution of the pressure gradient force term along the normal direction to the Lorentz force (see equation (2)). An outward moving MP ($v_{mp} = 70$ km/s estimated with 4-sc timing), consistent with Cluster going from MSH to MSPH, thus results in a very large positive contribution to Q which completely dominates the overall power conversion in equation (1). However, the model represents a nearly stationary MP and thus we can compare only the tangential contribution to Q in which both estimates corresponds to generators. Although, the model observes a lower magnitude of the power conversion, in this case by about a factor four.

4. Conclusions

[17] The comparison between BATS-R-US ideal MHD simulation and Cluster observations show that BATS-R-US can reproduce the detailed magnetic field and, to some extent, velocity observations from Cluster. BATS-R-US cannot reproduce the observed sharp MP transition region and also some topology shifts may occur, e. g. the expanded cusp region. BATS-R-US correctly predict the regions crossed by Cluster as a load and a generator region, correspondingly. The magnitudes of the energy conversion estimates across the MP from Cluster and BATS-R-US are in rather good agreement despite the limitations of discontinuities being a function of the grid resolution in global MHD simulations. The energy conversion estimated by $\vec{E} \cdot \vec{j}$ and $-\nabla \cdot \vec{S}$ in BATS-R-US are in good agreement for the

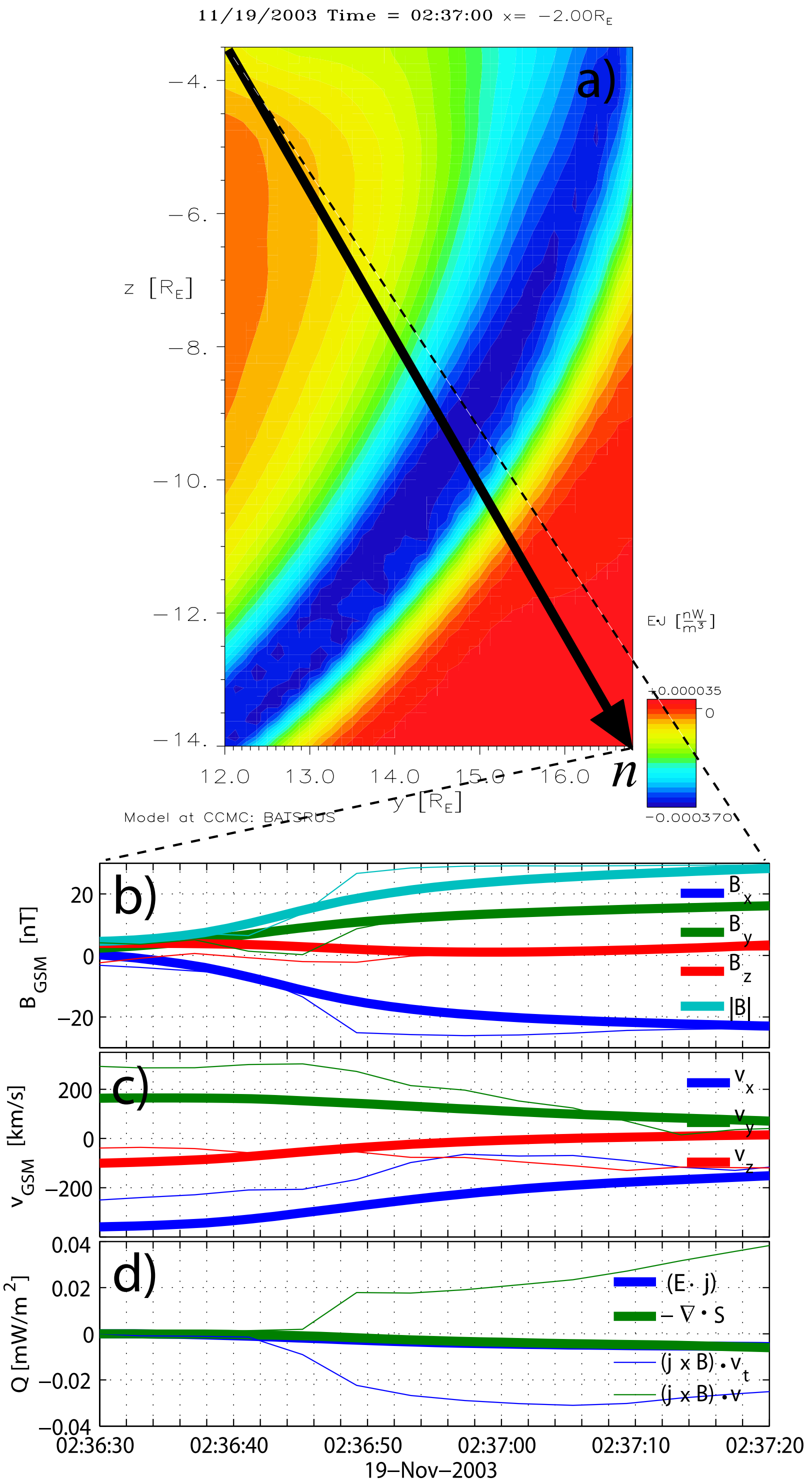

Figure 5. Same as Figure 3 but for the generator case.

generator case while they differ by a factor two for the load case most probably due to numerical dissipation effects in the MHD code. This difference should be investigated in more detail as it is important for the determination of which method to be used when estimating the energy conversion across the MP in regions of reconnection. Since the modeled MP is nearly static the model cannot take into account the energy conversion due to MP movement in the form of expansion or contraction of the MP or the existence of surface waves. However, Cluster MP crossings are almost always dynamic due to MP motion. This problem is particularly dominant when crossing regions of considerably different total magnetic field strength.

[18] **Acknowledgments.** Simulation results have been provided by the Community Coordinated Modeling Center at Goddard Space Flight

Center. The BATS-R-US Model was developed by the Center for Space Environment Modeling at the University of Michigan. LR is supported by the Swedish National Space Board. AV is supported by the Swedish Research Council.

References

Akasofu, S.-I. (1979), Energy coupling between the solar wind and the magnetosphere, *Planet. Space Sci.*, *27*, 425–431.

Escoubet, C. P., M. Fehringer, and M. Goldstein (2001), The Cluster mission, *Ann. Geophys.*, *19*, 1197–1200.

Gombosi, T. I., G. Toth, D. L. De Zeeuw, K. C. Hansen, K. Kabin, and K. G. Powell (2002), Semirelativistic magnetohydrodynamics and physics-based convergence acceleration, *J. Comput. Phys.*, *177*, 176–205.

Laitinen, T. V., M. Palmroth, T. I. Pulkkinen, P. Janhunen, and H. E. J. Koskinen (2007), Continuous reconnection line and pressure-dependent energy conversion on the magnetopause in a global MHD model, *J. Geophys. Res.*, *112*, A11201, doi:10.1029/2007JA012352.

Palmroth, M., T. I. Pulkkinen, P. Janhunen, and C.-C. Wu (2003), Storm-time energy transfer in global MHD simulation, *J. Geophys. Res.*, *108*(A1), 1048, doi:10.1029/2002JA009446.

Phan, T. D., et al. (2004), Cluster observations of continuous reconnection at the magnetopause under steady interplanetary magnetic field conditions, *Ann. Geophys.*, *22*, 2355–2367.

Powell, K. G., P. L. Roe, T. J. Linde, T. I. Gombosi, and D. L. De Zeeuw (1999), A solution-adaptive upwind scheme for ideal magnetohydrodynamics, *J. Comput. Phys.*, *154*, 284–309.

Rosenqvist, L., S. Buchert, H. Opgenoorth, A. Vaivads, and G. Lu (2006), Magnetospheric energy budget during huge geomagnetic activity using Cluster and ground-based data, *J. Geophys. Res.*, *111*, A10211, doi:10.1029/2006JA011608.

Rosenqvist, L., A. Vaivads, A. Retinò, T. Phan, H. J. Opgenoorth, I. Dandouras, and S. Buchert (2008), Modulated reconnection rate and energy conversion at the magnetopause under steady IMF conditions, *Geophys. Res. Lett.*, *35*, L08104, doi:10.1029/2007GL032868.

Weimer, D. R., D. M. Ober, N. C. Maynard, M. R. Collier, D. J. McComas, N. F. Ness, C. W. Smith, and J. Watermann (2003), Predicting interplanetary magnetic field (IMF) propagation delay times using the minimum variance technique, *J. Geophys. Res.*, *108*(A1), 1026, doi:10.1029/2002JA009405.

S. Buchert, L. Rosenqvist and A. Vaivads, Swedish Institute of Space Physics, Box 537, Lagerhyddsvagen 1, SE-751 21 Uppsala, Sweden. (lisa.rosenqvist@irfu.se)

I. Dandouras, CESR, 9 Ave. du Colonel Roche, F-31028 Toulouse CEDEX, France.

H. J. Opgenoorth, Solar System Mission Division, ESTEC, ESA, Keplerlaan 1, NL-2200 AG Noordwijk, Netherlands.

L. Rastaetter, Space Weather Laboratory, NASA Goddard Space Flight Center, Code 674, Greenbelt, MD 20771, USA.